Surgical and Radiologic Anatomy
https://doi.org/10.1007/s00276-024-03475-x

ORIGINAL ARTICLE

Mullan's triangle or anteromedial triangle of the middle cranial fossa: a cadaveric study with its surgical importance

Ariyanachi Kaliappan[1] · Rohini Motwani[1] · Mrudula Chandrupatla[1] · Apurba Patra[2]

Received: 23 July 2024 / Accepted: 22 August 2024

Abstract

Background Surgical approaches to the cavernous sinus (CS) and middle cranial fossa (MCF) can be challenging, particularly for young neurosurgeons. The anteromedial (Mullan's) triangle is a triangle by the side of the CS and constitutes part of the floor of the MCF. The contents include the sphenoid sinus, superior ophthalmic vein, and sixth cranial nerve. The literature contains very little research that has precisely defined and measured the anteromedial triangle while considering anatomical variances minimally.

Methodology The present study was conducted on the skulls of 25 adult human cadavers which were dissected to expose the anteromedial (Mullan's) triangle on both sides. After precisely defining the triangle on each side, measurements of the three borders were taken, and using Heron's formula, the area of each triangle was calculated.

Results On average, the length of the medial border was 12.5 (+3.1 mm); the length of the lateral border was 9.9 (+3.1 mm); the length of the base was 10.75 (+2.4 mm) and the area of the anteromedial triangle was 43.9 (+15.06 mm^2).

Conclusion Precise anatomical knowledge of the Mullan's triangle enables the treatment of disorders in often deformed anatomy or difficult-to-access structures. That is the reason it is important to gain a thorough understanding of the surgical anatomy and to adopt a safe procedure.

Keywords Anteromedial triangle · Cadaver · Cavernous sinus · Dimensions · Mullan's triangle

Introduction

As a result of its complex anatomy and potential risk to patients, cavernous sinus (CS) is referred to as a surgical "no-man's land." Dolenc and other pioneers' ground-breaking work signified a genuine revolution in surgical interest and understanding with reference to approaches to the CS [5].The skull base is a technically challenging region for neurosurgeons considering its location and important anatomical structures related to it. Around ten surgical triangles in the middle cranial fossa (MCF) close to the CS have been described in the literature (Fig. 1) [2, 13]. The boundaries of these triangles are often marked by the second (II) to sixth (VI) cranial nerves, which are crucial anatomical landmarks for the neurosurgeons. In the mid-1960s, Parkinson was the first to discover the first intracranial triangle formed in the lateral wall of the CS by the trochlear and ophthalmic nerves to safely access the internal carotid artery (ICA) lesion [11]. After then, a few anatomical and surgical investigations identified a number of triangles connected to the CS that are important for neurosurgeons. As they are based on constant anatomical landmarks, they serve as an intraoperatory pillar for localization of the CS and related structures.

Anteromedial triangle (AMT), also referred to as Mullan's triangle, as was first described by Mullan, in 1979 [10]. This triangle provides a limited corridor for visualising the final portion of the horizontal segment and the anterior bend of the ICA and sixth cranial (VI) nerve as it adopts a more inferolateral position towards ophthalmic nerve (V_1) and can be retracted medially for a greater amount of exposure [6]. AMT is also a corridor suited for exposing several other important structures, including the superior orbital vein, sphenoid sinus, and ophthalmic vein [3]. There are a very few studies in the literature that have clearly delineated and

✉ Rohini Motwani
rohinimotwani@gmail.com

[1] Department of Anatomy, All India Institute of Medical Sciences (AIIMS) Bibinagar, Hyderabad, Telangana, India

[2] Department of Anatomy, All India Institute of Medical Sciences (AIIMS), Bathinda, Punjab, India

Published online: 03 September 2024

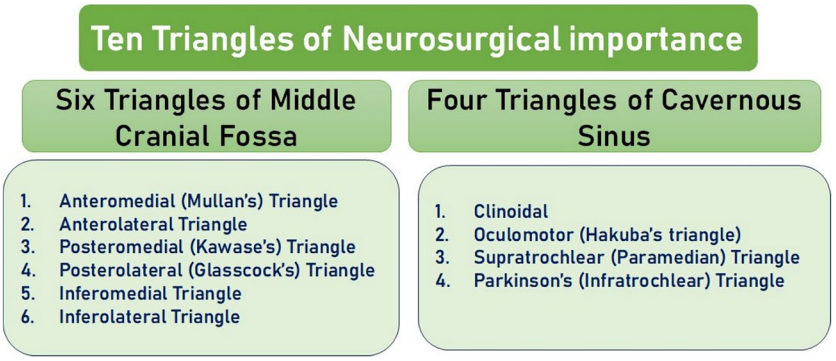

Fig. 1 Showing classification of the ten neurosurgical triangles of the middle cranial fossa and the cavernous sinus [2]

quantified the AMT. The AMT is bounded medially by posterior border of ophthalmic division (V_1) of trigeminal nerve (V), laterally by anterior border of maxillary nerve (V_2) and the base by a line connecting the superior orbital fissure to the foramen rotundum [10]. Carotid-cavernous fistulas can be accessed with further dissection within Mullan's space. A little amount of temporal retraction is required in order to expose this triangle during endoscopic surgery using the supraorbital extradural technique [9]. Some times, the superior orbital fissure artery passes through the lateral wall of the CS, supplying cranial nerves third (III), fourth (IV), sixth (VI), and ophthalmic nerve (V_1). The vascular supply of these nerves is therefore put at risk by procedures that alter the lateral wall of the CS at the anteromedial triangle, even if collaterals do exist [4]. Therefore, a comprehensive understanding of the structure and variations of the AMT is crucial to skull-based surgery; this knowledge facilitates surgical planning and the appreciation of regional pathology [1]. To date, only a few studies have examined and defined the boundaries of the AMT [16]. Additionally, it is essential to comprehend the AMT's dimensions in order to have a better understanding of the pathologic changes that exist inside and surrounding this region. Therefore, we anticipate that this study will aid neurosurgeons in their understanding of surgical approaches to the CS and MCF by providing with the additional information regarding the dimensions of the AMT.

Materials and methods

The present study was conducted on 25 donated adult human cadavers (13 females and 12 males) (Table 1), with age ranging from 75–80 years in the Department of Anatomy, All India Institute of Medical Sciences (AIIMS) Bibinagar, Hyderabad. Prior to their demise, all donors or their relatives gave their informed written consent, allowing their bodies to be employed in medical research and education. During the routine dissection and practical teaching of undergraduate medical students, after careful removal of brain, duramater overlying the floor of the MCF was removed with utmost care in order to expose underlying structures. To carry out the morphometric study of triangles of MCF, the trigeminal ganglion and its three divisions were preserved. Fine dissection was done to define the boundaries of the AMT on both the sides of the skull base in each of the 25 cadavers. The triangle was bounded medially by posterior border of the ophthalmic nerve (V_1) extending from its intersection with the medial margin of maxillary nerve to the lateral end of superior orbital fissure. The lateral boundary was formed by anterior border of the maxillary nerve (V_2), which was measured from its intersection with the mandibular nerve (V_3) to the anterior most end of the foramen rotundum. The base of the triangle was formed by an imaginary line joining the lateral end of superior orbital fissure to foramen rotundum (Figs. 2 and 3). The length of each border of the AMT was measured three times by the same author and the average was taken as final measurement (Table 3). All the measurements were made by the same author to avoid subjective variation. Measurements were taken with the help of geometric divider, keeping its pointed ends on the ends of margins to be measured (Fig. 4). Utmost care was taken to ensure that the exact distance between the pointed ends of the divider with which dimensions were measured on the specimen remain undisturbed while it was being transferred to the ruler for the measurements. With the help of Heron's formula, area of each triangle was calculated (as mentioned below) [8]. The results were statistically analyzed for mean, range and standard deviation. The student's t test was used to compare each parameter on the right and left side.

Table 1 Showing sex distribution of the cadavers used for the present study

Sex	Number of cadavers	Number of anteromedial triangles traced
Male	12	24
Female	13	26
Total	25	50

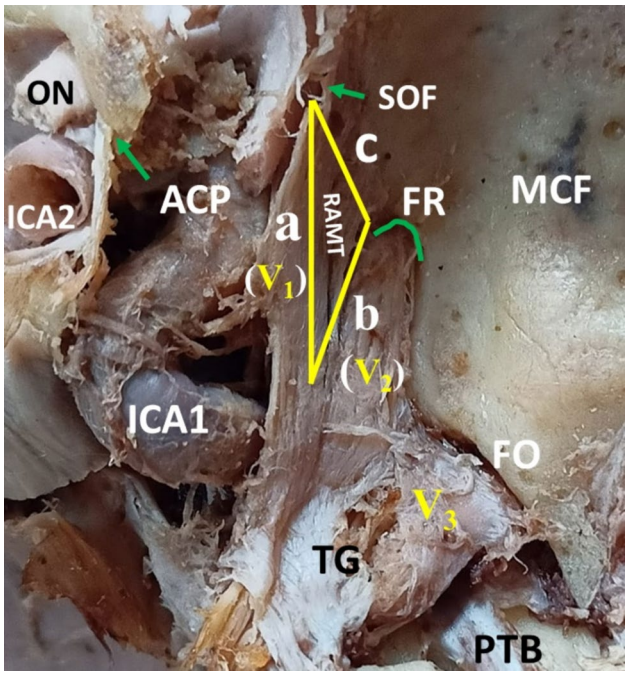

Fig. 2 Middle Cranial Fossa (MCF) of right side- superolateral view, showing Right Antero-Medial Triangle (RAMT) bounded by the ophthalmic division (**a-V_1**) of the trigeminal (V) nerve medially and the maxillary division (**b-V_2**) of the trigeminal (V) nerve laterally. The triangle base consists of the anterolateral wall of the bony Mi MCF formed by an imaginary line (‘**c**’) connecting the Superior Orbital Fissure (SOF) to the Foramen Rotundum (FR). V_3: Mandibular division of V nerve, ICA1: Internal Carotid Artery in cavernous sinus (Cavernous part), ICA2: Para clinoidal portion of Internal Carotid Artery (Cut end), ACP: Anterior Clinoid Process, FO: Foramen Ovale, ON: Optic Nerve, PTB: Petrous Temporal Bone, TG: Trigeminal Ganglion

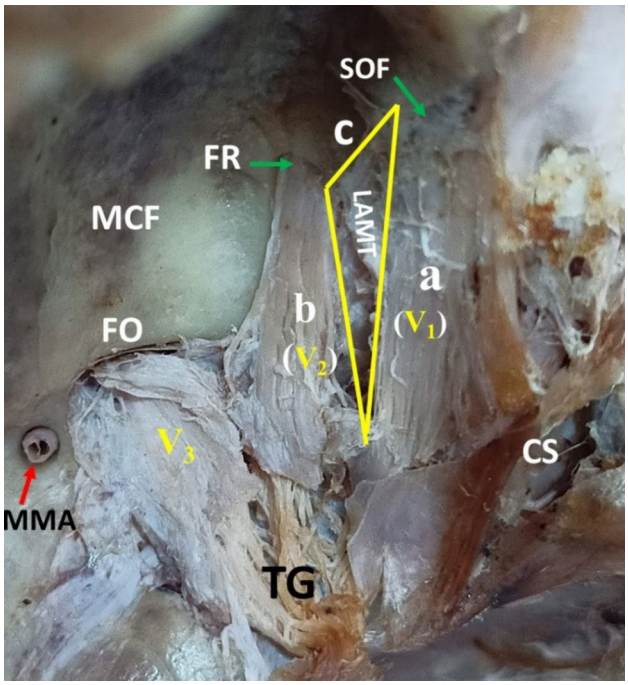

Fig. 3 Middle cranial fossa (MCF) of left side- superolateral view, showing Left Antero-Medial Triangle (LAMT), bounded medially by ‘**a’ (V_1)**: Ophthalmic nerve, laterally by ‘**b’ (V_2):** Maxillary nerve, **‘c’** forms the base of the triangle. CS: Cavernous Sinus, TG: Trigeminal Ganglion, MMA: Middle Meningeal Artery (cut end), SOF: Superior Orbital Fissure, FO: Foramen Ovale, FR: Foramen Rotundum

$$\text{Area, } A = \sqrt{s(s-a)(s-b)(s-c)}$$

Where,

$$S = \text{Semi Perimeter} = \frac{a+b+c}{2}$$

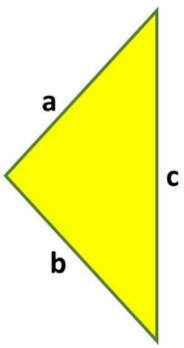

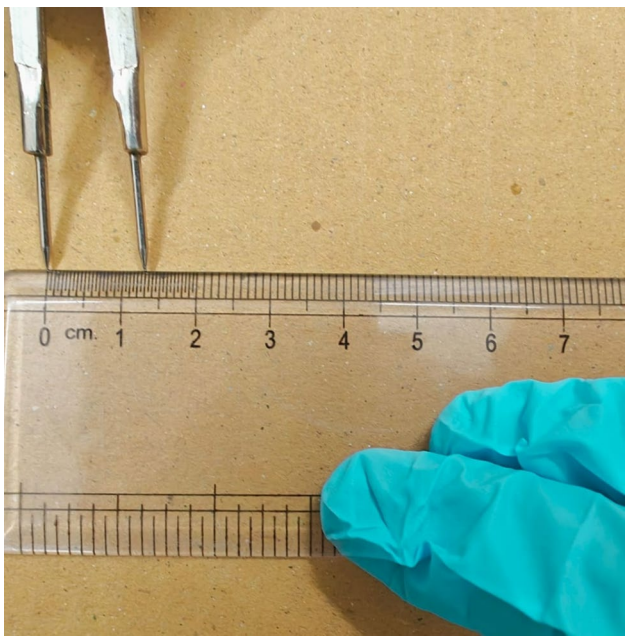

Fig. 4 Method used for measuring the boundaries of Anteromedial triangle of Middle Cranial Fossa, using geometric divider, keeping its pointed ends on the ends of margins to be measured

Results

The lengths of the medial border [along the ophthalmic nerve (V_1)] ranged from 8.5 mm to 25 mm, with a mean length and standard deviation of 14.86 mm and 4.51 mm respectively. The lengths of the lateral border [along the maxillary nerve (V_2)] ranged from 5 to 17 mm, with a mean length and standard deviation of 9.8 mm and 3.4 mm respectively. The lengths of the base (from lateral end of superior orbital fissure to foramen rotundum) ranged from 7 to 21 mm, with a mean length and standard deviation of 13.17 mm and 4.16 mm respectively. The area of the AMT observed was 57.44 ± 35.2 mm^2 (Table 2). In the 25 formalin fixed cadavers dissected, no statistically significant difference was observed in the measurements related to the boundaries of the AMT of the CS between the right and the left side ($p > 0.05$) (Table 3).

Discussion

Endovascular and radiosurgery are becoming more and more popular in advanced brain surgery owing to great degree of safety and short recovery periods. It is crucial to have a thorough understanding of CS or MCF triangles. Even when CS lesions—whether malignant or vascular—distort the typical anatomy, identifying this distortion requires a foundational understanding of the normal architecture around the CS and in MCF. The ability to accurately identify essential landmarks during the dissection of anatomical corridors in intra-cavernous aneurysms remains unaffected, despite the possibility of a high degree of anatomical distortion in certain cases of CS neoplasia. The surgeon also has to be aware that manipulating the cranial nerves might cause the triangles to expand. Regarding the authors' methodology, we are clarifying three points; two have to do with measurements, and one with nomenclature. To prevent bias, all measurements were taken by the same author. When all three sides of a triangle are known, the area may be easily calculated using the Heron's formula. The authors followed Rhoton's naming scheme when referring to the nomenclature of the triangle [14].

In the present study, the length of the medial border observed was 14.86 ($\pm$4.51) mm; the length of the lateral border was 9.8 ($\pm$3.4) mm; the length of the base was 13.17 ($\pm$4.16) mm and the area of the AMT calculated was 57.44 ± 35.2 mm^2. To the best of our knowledge, no cadaveric studies have been done on the dimensions of AMT except by Watanabe et al., and Isolan et al. [7, 17] who measured the dimensions of AMT in 12 tissue blocks containing bilateral CS and 18 CS of five cadaveric heads and four skull bases respectively. To our knowledge, this is the first Indian study aimed at defining the measurements of the AMT.

In the study done by Watanabe et al., the mean length of the medial border [along ophthalmic nerve (V_1)], lateral border [along maxillary nerve (V_2)] and the base are 7.8 mm, 5.83 mm and 12.0 mm respectively with the lateral border being the longest and the shortest border along the maxillary nerve [17]. This contradicts our findings where the longest border of the triangle extends along the ophthalmic nerve (V_1). Isolan et al., documented the mean length of the medial [along ophthalmic nerve [V_1)], lateral border [along maxillary nerve [V_2)] and base as 10.18 ± 0.62 mm, 7.87 ± 0.29 mm and 9.96 ± 1.13 mm and respectively and the area of the triangle is 36.26 ± 3.75, the findings of whom are almost similar to our study with the ophthalmic nerve (V_1) located along the lengthier side of the triangle [12]. The comparison table for the morphometry of AMT is given in Table 4.

Surgeons can better plan their approach to the MCF by using the AMT. It serves as a guide for locating important channels and structures inside the skull base, facilitating the safe movement of surgical tools. Accurate identification and understanding of this anatomical area help in reducing the risk of complications associated with surgeries in the cranial base, such as injury to vital nerves and blood vessels. Also the AMT serves as a useful teaching tool for medical students and residents learning about cranial anatomy and surgical approaches [4].

We hypothesize that the base of these measurement variations may be varying degrees of dissection of the ophthalmic and maxillary nerves as well as the force applied when retracting the duramater over the MCF. In the future, the cadaveric results should be coupled with the radiological data to enable efficient identification of appropriate surgical approaches to the MCF across this key corridor, therefore overriding the subjective variations that will inevitably arise during the dissection. The AMT provides a narrow corridor that allows visualization of the final portion of the horizontal segment and the anterior bend of the cavernous part of ICA and sixth cranial nerve as it assumes a more inferolateral position towards ophthalmic nerve that can be medially retracted for better exposure [5]. Additionally, by drilling the bone between the foramen rotundum and the superior orbital fissure, the sphenoid sinus is left accessible [4].

Limitations

Studies suggest that 10% to 15% of tissue shrinkage is caused by formalin, which may conceal the original dimensions[15]. However, according to another study conducted

Table 2 Showing measurements of Anteromedial triangles of both the sides in human cadavers

Specimen Number	Sides	Medial border (mm) [along V1]	Lateral border (mm) [along V2]	Superior orbital fissure to foramen rotundum [Base] (mm)	Area of the triangle (mm^2)
1	Right	18	17	9	75.63
	Left	18	13	11	70.99
2	Right	9	10	8	34.20
	Left	10	10	10	43.30
3	Right	15	8	11	42.89
	Left	17	8	11	35.50
4	Right	11	6	9	26.98
	Left	11	8	10	38.53
5	Right	10	8	11	38.53
	Left	16	7	13	44.50
6	Right	14	9	7	26.83
	Left	15	7	7	16.89
7	Right	15	9	13	58.16
	Left	15	9	19	66.08
8	Right	16	8	13	51.68
	Left	15	7	12	41.23
9	Right	14	7	8	18.79
	Left	17	6	8	16.67
10	Right	10	7	11	34.29
	Left	9	8	12	35.99
11	Right	10	16	11	54.3
	Left	9.5	15	12	56.9
12	Right	11.5	14	7	40.08
	Left	11	14.5	11	59.98
13	Right	8.5	8.5	10	34.37
	Left	9.5	9.5	10.5	41.57
14	Right	9	13	11.5	50.55
	Left	9	13	11	48.80
15	Right	10	11	13	53.44
	Left	11	11.5	12.5	58.42
16	Right	15	5	16	37.47
	Left	17	5	18	42.42
17	Right	18	12	13	77.95
	Left	20	13	20	122.94
18	Right	15	5	17	36.21
	Left	16	6	12	27.66
19	Right	17	7	20	57.45
	Left	17	7	17	58.23
20	Right	21	13	18	116.27
	Left	22	13	17	110.31
21	Right	20	12	21	117.20
	Left	20	10	15	72.62
22	Right	12	5	9	20.40
	Left	13	9	12	52.15
23	Right	23	12	13	56.28
	Left	23	12	20	119.94
24	Right	25	16	21	167.03
	Left	25	17	21	176.56

Table 2 (continued)

Specimen Number	Sides	Medial border (mm) [along V1]	Lateral border (mm) [along V2]	Superior orbital fissure to foramen rotundum [Base] (mm)	Area of the triangle (mm^2)
25	Right	15	7	20	42
	Left	15	6	16	44.98
	Mean ± SD ($n = 30$)	14.86 ± 4.51	9.8 ± 3.4	13.17 ± 4.16	57.44 ± 35.2
	Range (mm)	8.5—25	5—17	7—21	16.67 – 176.56

Table 3 Comparison of measurements of the Anteromedial triangles between the right and left sides

	Side	Mean ± SD (mm) ($n = 30$)	Range (mm)	*P*-value
Medial border (along V1)	Right	14.48 ± 4.5	8.5–25	0.55
	Left	15.24 ± 4.5	9–25	
Lateral border (along V2)	Right	9.82 ± 3.6	5–17	0.96
	Left	9.78 ± 3.3	5–17	
Superior orbital fissure to foramen rotundum [base]	Right	12.82 ± 4.4	7–21	0.55
	Left	13.52 ± 3.9	7–21	

SD Standard deviation, *n* number of samples.

In the 25 formalin fixed cadavers dissected, no statistically significant difference was observed in the measurements related to the boundaries of the Anteromedial triangles of the middle cranial fossa between the right and the left side ($P > 0.05$)

Table 4 Comparison of the morphometry of Anteromedial triangle of present study with similar other studies

S.No	Authors	Number of specimens	Observations
1	Watanabe et al., [11]	12 Japanese cadaveric heads (24 cavernous sinus)	Medial border (along V1): 7.8 mm Lateral border (along V2): 5.83 mm Base (from SOF to foramen rotundum): 12 mm
2	Isolen et al. [12],	9 cadaveric heads (18 cavernous sinus) and 4 skull bases	Medial border (along V1): 10.18 ± 0.62 mm Lateral border (along V2): 7.87 ± 0.29 mm Base (from SOF to foramen rotundum): 11.59 ± 1.61 mm
3	Present study	25 adult cadaveric heads (50 cavernous sinus)	Medial border (along V1): 14.86 ± 4.51 mm Lateral border (along V2): 9.8 ± 3.4 mm Base (from SOF to foramen rotundum): 13.17 ± 4.16 mm Area: 57.44 ± 35.2 mm^2

on breast cancer specimens, there was no discernible difference between the fresh and fixed specimens in 96% of the cases [12].

Conclusion

Because the CS triangles are natural passageways that allow lesions inside the CS to be accessed, their normal anatomy and size are significant for approaches to CS lesions. In endoscopic endonasal procedures, the triangle is an essential window for accessing MCF structures. Understanding these anatomical corridors and their corresponding sizes is essential for identifying the lesions and preventing damage to the neurological and vascular structures. We hope that our findings will deepen the comprehension of this crucial surgical triangle and related structures in anatomy education, radiology and surgical training.

Acknowledgements We would like to thank the donors and their families for agreeing to donate the bodies of their loved ones for medical education and research purposes. We are grateful to the dissection hall attenders in our department for their technical assistance.

Author contributions Conceptualization: AK, RM, MC; Data acquisition: AK, RM, MC, AP; Data analysis or interpretation: AK, RM, MC. Drafting of the manuscript: AK, RM, MC. Critical revision of the manuscript: AK, RM, MC, AP. Approval of the final version of the manuscript: all authors.

Funding Nil.

Data availability No datasets were generated or analysed during the current study.

Declarations

Conflicts of interest The authors declare no competing interests.

Ethical approval and consent to participate This is a cadaveric study that is completely done on donated cadavers, used for teaching and research purpose. All donors or their relatives provided informed written consent prior to their death so that their bodies can be utilized for medical education and research. As the study was conducted on donated cadavers, exemption from review was taken from Institutional Ethics Committee (IEC).

Consent for publication All the authors gave consent for the publication of the report.

References

1. Bayatli E, Cömert A (2023) Scratching in the minefield: using intertriangles line to safely perform anterior petrosectomy. Surg Radiol Anat 45:513–522. https://doi.org/10.1007/s00276-023-03131-w
2. Chavez-Herrera VR, Campero Á, Ballesteros-Herrera D et al (2023) Microsurgical and illustrative anatomy of the cavernous sinus, middle fossa, and paraclival triangles: a straightforward, comprehensive review. Surg Radiol Anat 45:389–400. https://doi.org/10.1007/s00276-023-03105-y
3. Conti M, Prevedello DM, Madhok R, Faure A, Ricci UM, Schwarz A et al (2008) The antero-medial triangle: the risk for cranial nerves ischemia at the cavernous sinus lateral wall. Anatomic cadaveric study Clin Neurol Neurosurg 110(7):682–686
4. Dalgiç A, Boyaci S, Aksoy K (2010) Anatomical study of the cavernous sinus emphasizing operative approaches. Turk Neurosurg 20(2):186–204
5. Dolenc V. (1989) Anatomy and Surgery of the Cavernous Sinus. 1st ed. Vienna, Austria: Springer-Verlag
6. Dolenc VV (1985) A combined epi- and subdural direct approach to carotid-ophthalmic artery aneurysms. J Neurosurg 62(5):667–672
7. Isolan GR, Krayenbühl N, de Oliveira E, Al-Mefty O (2007) Microsurgical anatomy of the cavernous sinus: measurements of the triangles in and around it. Skull Base 17(6):357–367
8. Kaliappan A, Motwani R, Chandrupatla M (2024) Anterolateral surgical triangle of the cavernous sinus: a cadaveric study of neurosurgical importance. Surg Radiol Anat 46:41–46. https://doi.org/10.1007/s00276-023-03261-1
9. Komatsu F, Komatsu M, Inoue T, Tschabitscher M (2011) Endoscopic supraorbital extradural approach to the cavernous sinus: a cadaver study. J Neurosurg 114(5):1331–1337
10. Mullan S (1979) Treatment of carotid-cavernous fistulas by cavernous sinus occlusion. J Neurosurg 50(2):131–144
11. Parkinson D (1965) A surgical approach to the cavernous portion of the carotid artery. Anatomical studies and case report. J Neurosurg 23(5):474–483
12. Pritt B, Tessitore JJ, Weaver DL, Blaszyk H (2005) The effect of tissue fixation and processing on breast cancer size. Hum Pathol 36(7):756–760
13. Rhoton AL (2002) The cavernous sinus, the cavernous venous plexus, and the carotid collar. Neurosurgery 51(4):S375-410
14. Rhoton AL (2002) The supratentorial cranial space: microsurgical anatomy and surgical approaches. Neurosurgery 51:S1-iii
15. Siu KF, Cheung HC, Wong J (1986) Shrinkage of the esophagus after resection for carcinoma. Ann Surg 203(2):173–176
16. Stempniewicz M, Sloniewski P, Smida K, Rynkowski M, Zielinski P (2001) The microsurgical anatomy of the anteromedial triangle of the cavernous sinus. Research gate 1:11
17. Watanabe A, Nagaseki Y, Ohkubo S, Ohhashi Y, Horikoshi T, Nishigaya K et al (2003) Anatomical variations of the ten triangles around the cavernous sinus. Clin Anat N Y N 16(1):9–14